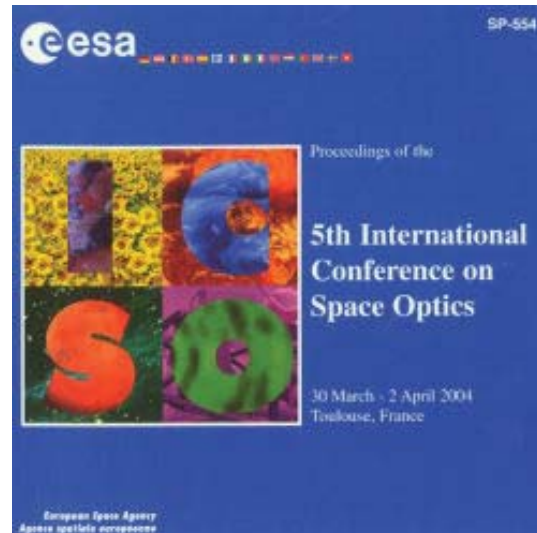


# International Conference on Space Optics—ICSO 2004

Toulouse, France

30 March–2 April 2004

*Edited by Josiane Costeraste and Errico Armandillo*



## *HRS camera: a development and in-orbit success*

*Gilles Planche, Christian Massol, Laurent Maggiori*



International Conference on Space Optics — ICSO 2004, edited by Errico Armandillo,  
Josiane Costeraste, Proc. of SPIE Vol. 10568, 105680K · © 2004 ESA and CNES  
CCC code: 0277-786X/17/\$18 · doi: 10.1117/12.2307977

## HRS CAMERA: A DEVELOPMENT AND IN-ORBIT SUCCESS

Gilles Planche <sup>(1)</sup>, Christian Massol <sup>(2)</sup>, Laurent Maggiori <sup>(3)</sup>

<sup>(1)</sup>, ASTRUM, 31, Rue des Cosmonautes, 31402 Toulouse Cedex 4, France, gilles.planche@astrium.eads.net

<sup>(2)</sup>, ASTRUM, 31, Rue des Cosmonautes, 31402 Toulouse Cedex 4, France, christian.massol@astrium.eads.net

<sup>(3)</sup> Spot Image 5, Rue des Satellites, BP 4359, F-31030 Toulouse Cedex, France, laurent.maggiori@spotimage.fr

### KEYWORDS:

Stereoscopy, DEM (Digital Elevation Model), HRS (High Resolution Stereoscopic instrument), SPOT 5 satellite

### ABSTRACT

Embarked on-board SPOT5, the French Earth Observation Satellite, the High Resolution Stereoscopic (HRS) camera, dedicated to simultaneous acquisition of stereo pairs with 60 km x 120 km wide swath and 10 m spatial resolution create Digital Elevation Models (DEM) with 10 m elevation accuracy. After on year in-orbit, the instrument exhibits excellent performances. Mainly built around two dioptric optics arranged with a 40° angle, which optimises the elevation performances, the HRS camera was developed in one shot, direct qualification and validation on flight model. After a description of HRS instrument architecture, design and performances, this paper describes its development and on-ground verification results. Then, the elevation in-orbit accuracy performances and the DEM end-products are presented.

## 1. HRS INSTRUMENT

### 1.1. Mission

The HRS mission is to generate Digital Elevation Model (DEM), geographical maps that include the altitude information, from stereoscopic pairs of images acquired sequentially by the High Resolution Stereoscopic HRS instrument mounted on SPOT5 satellite.

To satisfy defence, institutional cartography, geographical information system, telecommunication markets<sup>1</sup>, the HRS mission is sized to acquire 30 millions km<sup>2</sup> over 5 years with 10 m elevation accuracy.

### 1.2. Instrument principle and dimensioning

Based on a push-broom concept with a wide optical field of view, the HRS instrument acquires each image of the stereo pair from:

- A row scanning obtained by the reading of a 12000 pixels CCD detector with a 10 m pixel resolution
- A column scanning obtained by the satellite velocity over its orbit. Thanks to the frequency sampling, the resolution is 5 m on this axis.

Stereo pairs are acquired along track in panchromatic spectral band [0.48µm - 0.7µm] by two cameras (fore and aft cameras), tilted by ± 20° with respect to Nadir

about the track direction to ensure a 0.8 B/H ratio that optimises the elevation accuracy. SPOT5 being located at 830 km altitude, 600 km length of stereo strips is ensured, two consecutive stereo strips being spaced by 600 km as illustrated on Fig.1. To access any point on the earth surface within the orbital cycle without out-of-track sighting capability, selected for design simplicity reasons, the track width is greater than 109 km.

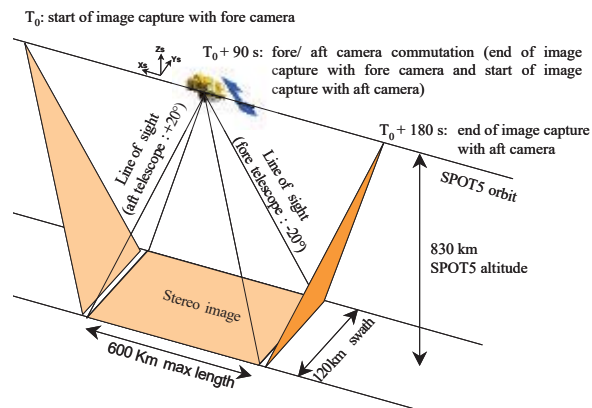


Fig.1: HRS imaging scenario

Getting excellent elevation accuracy is only possible with good radiometric and image finesse performances. Therefore, Modulation Transfer Function (MTF) characterizing the image quality and signal over noise ratio are of prime importance for the DEM accuracy and drive the instrument design and performances.

Table1: HRS imaging characteristics

Parameters	Characteristics
Nb of pixels /row	12000
Ground sampling	Row, 10 m Column, 5 m
Swath Width	120 km
Viewing angle	-20° (fore camera) +20° (aft camera)
Spectral panchromatic range	0.48 µm - 0.70 µm
Min observable luminance	L1 = 19 (W.m <sup>-1</sup> .sr <sup>-1</sup> .µm <sup>-1</sup> )
Max observable luminance	L4 = 379 (W.m <sup>-1</sup> .sr <sup>-1</sup> .µm <sup>-1</sup> )

### 1.3. Architecture and functions

The architecture of HRS instrument, briefly illustrated on the diagram hereunder, provides the following functional subassemblies:

#### Optical Assembly

Mounted on the instrument structure via quasi-isostatic mounts, 2 cameras, oriented at  $+20^\circ/-20^\circ$  with respect to Nadir, ensure the optical imaging and spectral filtering, the signal detection and video generation.

Each camera is composed of a detection unit coupled to a refractive telescope that provides the image quality and the focusing on the CCD detector thanks to a 11 lenses optical combination. Two parallel blades on the telescopes front side realize the spectral filtering and the radiation shielding (SUPRASIL blade). The telescope focus, key optical quality parameter, is thermally compensated and controlled. The telescope characteristics are:

- Focal distance: 580 mm
- Useful optical diameter: 150 mm

Based on a Thomson TH 7834 CCD (12000 pixels of  $6,5 \times 6,5\mu\text{m}^2$ ) and its proximity electronics, the detection unit is directly mounted on the rear side of the telescopes to ensure the focus stability performance. In this configuration, the CCD, controlled at  $24^\circ\text{C}$ , is thermally and mechanically coupled to the telescopes. The proximity electronics dissipated power is evacuated thanks to specific radiators mounted on the top of the detection units. The detection unit sequencing and the acquisition of the video signal is performed by the MVS (Module Video Stereo).

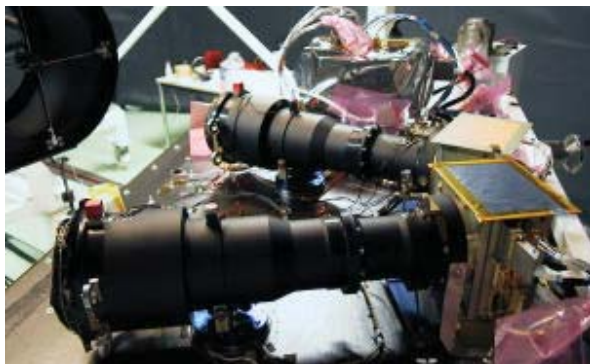


Fig.2: HRS telescopes during integration and alignment on the main structure

#### Structures

Ultra light and highly stable, the main structure, made of Al honeycomb / CFRP sandwich, featuring new cyanate material (low thermal and moisture expansion figures), ensures a stable accommodation of the instrument units and decoupled interfaces with the satellite. In addition, secondary structures are implemented to support the active thermal control (MVS and Optical Assembly thermal hoods) and to avoid sun entrance in the cameras (sun cap).

#### Thermal control

The Optical Assembly accurate thermal control ( $\pm 0,5^\circ\text{C}$  temperature and thermal gradient stabilities), avoiding the use of any refocusing mechanism, is achieved thanks to a thermal enclosure concept that radiatively controls the high thermal inertia assembly via a combination of active and passive thermal control.

#### Instrument control electronics

Accommodated inside a single unit, the instrument control electronics (MVS) provides management, housekeeping, detection sequencing and video electronics.

The management and housekeeping electronics realize the implementation of instrument modes and monitoring, the active heat control of the instrument and the standard SPOT5 interfaces with the satellite (DC/DC conversion of the satellite power bus and OBDH data handling bus). A CCD sequencing electronics, a Video electronics at  $4,1\text{Mpixels.s}^{-1}$ , capable of up to  $10\text{Mpixels.s}^{-1}$  and a 12 bits analog to digital conversion complete the detection chain and provide HRS images digital information to the satellite.

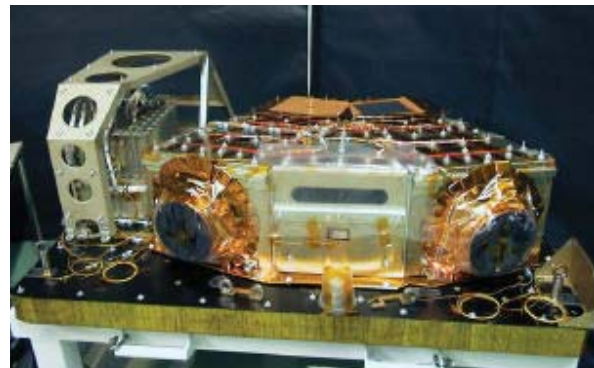


Fig.3: HRS instrument fully integrated (MLI not shown)

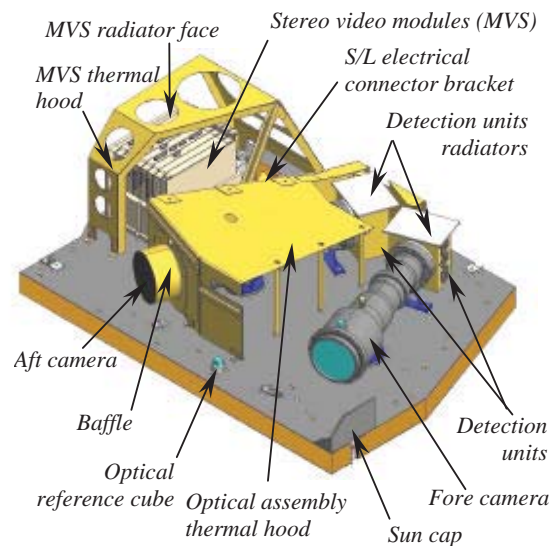


Fig.4: HRS exploded view

### 1.4. Accomodation on SPOT5

HRS instrument accommodation on SPOT5 is driven by two main considerations: on one hand, the maximization of interfaces decoupling between SPOT5 and HRS instrument and on the other hand, the minimization of the mechanical path between HRG and HRS instruments to optimise their relative stability. Thermal isolation (MLI, thermal washers) is implemented at instrument interfaces. Mechanical decoupling is achieved via isostatic mounts used on sensitive instrument units (cameras).

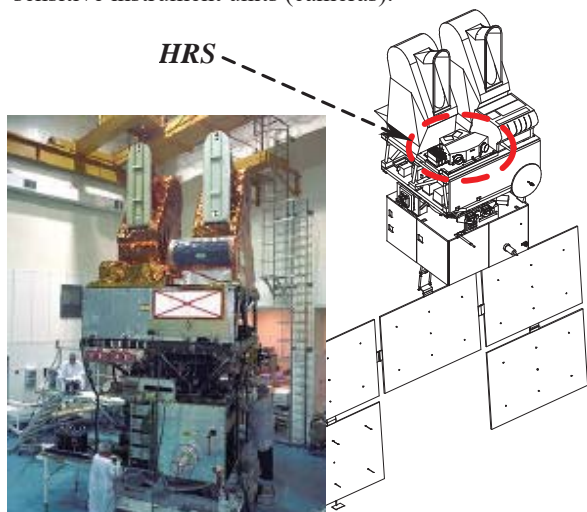


Fig.5: HRS on the earth side of SPOT5 satellite

### 1.5. Main performance data

HRS performances deal with:

- Geometrical performances:
  - Alignment stability between cameras
  - Alignment stability between each camera and the instrument alignment reference
- Radiometric performances
  - Signal over noise ratio
  - Linearity, Resolution, Dispersion
- Optical performances
  - MTF
  - Straylight, Polarisation, Transmission

Table2: Main instrument performances requirements

Functional performances		Comments
Alignment stability	< 150 $\mu$ rad	Between cameras
	< 500 $\mu$ rad	Between each camera and optical reference
S/B ratio	> 130 @ L2	$L2 = 118 \text{ W.m}^{-1}.\text{sr}^{-1}.\mu\text{m}^{-1}$
MTF	> 0,18	Across Track
	> 0,20	Along Track
Mass	< 90 kg	
Power	< 75 W	Consumption in imaging mode
Reliability / availability	> 0,98	For the nominal mission

## 2. DEVELOPMENT AND VERIFICATION

### 2.1. Instrument development

#### Timescale

Decision to implement HRS mission on SPOT5 was finalised in the very beginning of year 1999 with the major condition that HRS development should not delay the overall satellite timescale. This resulted in an overall timescale for HRS instrument development of 2 years.

#### Development logic

Given the available time, it was necessary to start in parallel units and instrument studies during the early engineering phase and to select a mono model philosophy, direct manufacturing of proto-flight model. Therefore, the instrument development was split in three phases, as illustrated on Fig.6:

- Architecture and design phase (from  $T_0$  to  $T_0+5$ ), concluded by a Preliminary Design Review
- Consolidation phase (from  $T_0+5$  to  $T_0+15$ ), concluded by a Manufacturing Release Review
- Qualification phase (from  $T_0+15$  to  $T_0+25$ ), concluded by a Qualification Review

The early engineering phase was an essential step for the success of the HRS challenging development. Indeed, to speed up the instrument definition, concurrent engineering was implemented with joint teams working in parallel to early identify design drivers and freeze the architecture, the design and the interfaces of the overall instrument. This phase has led to develop in parallel all mathematical models, to run simulations and establish budgets, each industrial team being fed in quasi real time by the others' study outputs.

For the same schedule constraints reasons, bulk of HRS instrument electronics are made of Mil standard parts, with adequate screening. Extensive use of Field Programmable Gate Array (FPGA) components for digital electronics allowed simple, late and quick design evolution. At satellite interface level, full « High-Rel » standard components are used.

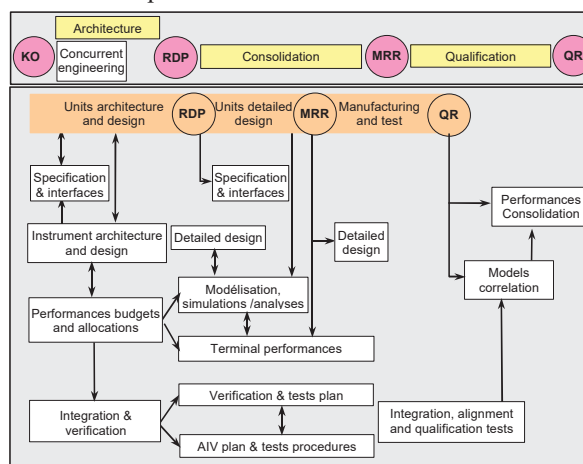


Fig.6: HRS development logic

## 2.2. Instrument verification

### Verification logic

Combination of analyses, simulations and tests, HRS verification and qualification programme was successfully held in 2000. However, the full qualification and the instrument flight worthy ability was only pronounced in 2001 after successful EMC qualification performed at S/L level.



Fig.7: HRS in vacuum chamber during TB/TV tests

The verification programme, done at instrument level, followed the following sequence:

- *Instrument alignment:* fore wrt aft camera alignment and alignment of cameras wrt alignment reference
- *Functional and performances tests at ambient:* modes management, thermal control, geometrical, radiometric and optical performances
- *Reference test:* sub-set of functional and performances parameters verification to trend the instrument health up to launch
- *Mechanical qualification:* mass and design qualification under mechanical environment (QSL, sine and acoustic environment)
- *Thermal qualification:* thermal power, thermal control and instrument performances verification under TB/TV environment. It is to be mentioned that a specific defocus sequence was applied during this test to characterise the defocus model

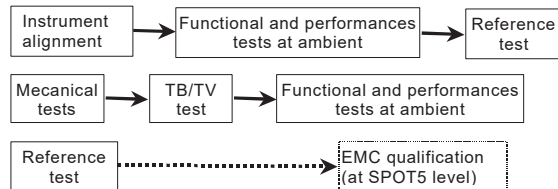


Fig.8: HRS verification sequence

### Verification results

#### Geometrical performances

After a characterization of reference frames transfer matrices, the alignment stabilities (geometrical performances) were trend during the instrument verification sequence (before and after mechanical and thermal environment).

The results, illustrated on Table3, highlighted excellent stability performances that allow for automatic data reduction at customer level.

Table3: Alignment stabilities verification

	Aft camera / optical ref	Fore camera / optical ref	Between cameras
After vibration	< 85 $\mu$ rad	< 55 $\mu$ rad	< 125 $\mu$ rad
After TB/TV	< 115 $\mu$ rad	< 30 $\mu$ rad	< 85 $\mu$ rad

#### Radiometric performances

After video chain calibration, mainly dedicated to gain and phase settings, the functional radiometric behaviour was first measured, especially:

- CCD offset correction
- Video chain behaviour in case a instrument detector saturation
- Recovery period (less than one CCD line) when switching from one camera to the other one or when changing the gain of the video chain

Then, the radiometric coefficients (equalization and dark coefficients) necessary to compensate for telescope and detection chain non-uniformity were characterized and delivered to the customer. Finally, the radiometric performances measured at ambient and under vacuum, exhibited excellent results in all domains.

Table4: Radiometric performances verification results

	Specification	Measures
Dispersion	Global	< 15 %
	Local	< 8 %
Noise	S/N @ L2	> 120
Linearity	Relative @ G3	< 2 %

As illustrated on Fig.9, the noise under different brightness, main instrument radiometric performance, is well within the specifications

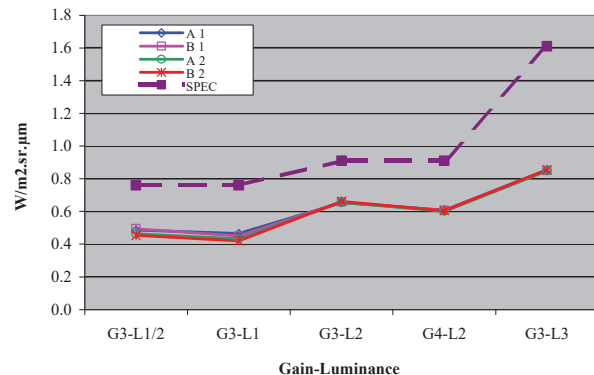


Fig.9: Noise versus brightness

HRS detection chain is linear over the large dynamic range (see Fig.10).

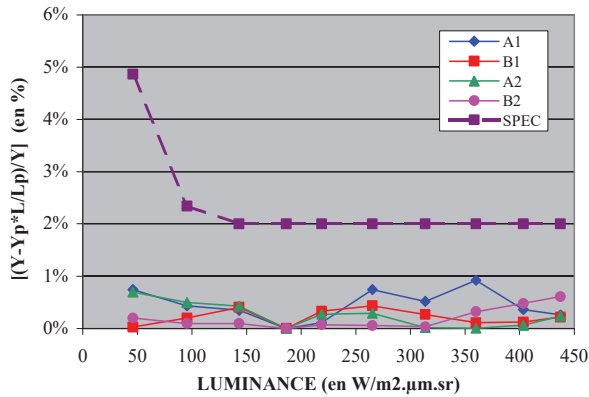


Fig.10: Relative linearity@ G3

**Optical performances**

Spectral response, straylight, polarisation, distortion and Modulation Transfer Function (MTF) are the main optical performances, which have driven the instrument design. Measured at ambient and under vacuum (especially MTF), these performances are illustrated on Table4.

Table4: Optical performances verification synthesis

	Measures	Comments
<b>Transmission</b>	0.55	
<b>Rejection</b>	< 0.1 %	Rejection: transmission outside spectral range
<b>Straylight</b>	< 10 %	Worst case figure when light is rasante
<b>Polarisation</b>	< 0.3 %	
<b>Distortion</b>	< 15 µm	Without correction modelling
<b>MTF</b>	> 0.19 > 0.26	Fore camera Aft camera

HRS mission and elevation accuracy are very dependent of instrument MTF performances. Therefore, during the instrument verification sequence, a specific attention was paid to this critical parameter that includes the MTF over the Field of View at best focus and the defocus performances. Although well within the specification for both cameras, a better MTF performance is observed on camera2 (Fig.12) compared to camera1 (Fig.11). This is only due to the dioptric telescope lenses alignment procedure, largely improved on the second camera to reduce the residual astigmatism. Therefore, complying with MTF requirement means a defocus stability of ± 30 µm on camera 1 (fore camera) and ± 45 µm on camera2 (aft camera).

So, it is clear that focus alignment and stability and, consequently the thermal control of the cameras, are key issues for the HRS mission performances. Therefore, large efforts were spent to master the defocus stability performance.

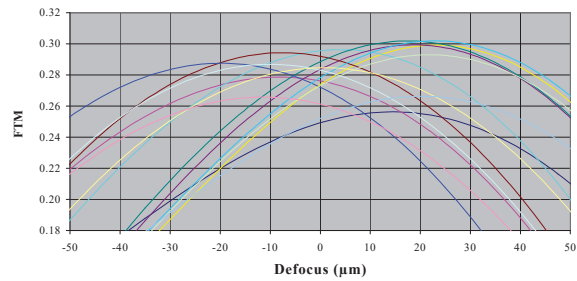


Fig.11: Fore camera MTF over the Field of View

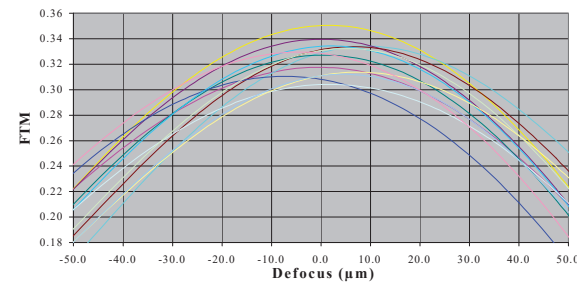


Fig.12: Aft camera MTF over the Field of View

Thanks to optical simulations, a defocus modelling was first established:

$$\Delta f = \Delta f_i + S_{\theta_o} * \theta_o + S_{G_l} * G_l + S_{\theta_B} * \theta_B + S_{\theta_{hs}} * \theta_{hs} + S_{\theta_{hsw}} * \theta_{hsw}$$

with:

- $\Delta f_i$  : Initial focus adjustment @ 0°C
- $S_{\theta_o}$  : Sensitivity to camera mean temperature
- $S_{G_l}$  : Sensitivity to camera longitudinal gradient
- $S_{\theta_B}$  : Sensitivity to baffle temperature
- $S_{\theta_{hs}}$  : Sensitivity to heat sink of the observed scene
- $S_{\theta_{hsw}}$  : Sensitivity to orbital variation of heat sink
- $\theta_o$  : Camera mean temperature
- $G_l$  : Camera longitudinal gradient
- $\theta_B$  : Baffle temperature
- $\theta_{hs}$  : Heat sink of the observed scene
- $\theta_{hsw}$  : Orbital variation of heat sink

Then, to correlate the model and predict flight performances, defocus sensitivity cases were introduced during TB/TV test. These specific technological cases performed on both cameras allowed estimating the model coefficients with defocus accuracy better than 4 µm over the whole campaign:

- $\Delta f_i$  : - 87 µm (camera1) and - 79 µm (camera2)
- $S_{\theta_o}$  : + 7 µm/°C                       $S_{\theta_{hs}}$  : -0.7 µm/°C
- $S_{G_l}$  : + 8.6 µm/°C                       $S_{\theta_{hsw}}$  : + 0.43 µm/°C
- $S_{\theta_B}$  : - 2.2 µm/°C

Referring to Fig. 11 and 12 and the estimated in-orbit defocus, [-15 µm; +11 µm] at 1σ and [-28 µm; +24 µm] at 2σ, the MTF performances at 2σ are:

- Camera1: MTF > 0.19
- Camera2: MTF > 0.26

### 3. HRS IN-ORBIT RESULTS

#### 3.1. HRS technological monitoring

After one year of successful mission in orbit, HRS instrument presents stable and excellent performances on observable parameters:

- Voltage, current and power consumption
- Temperatures
- Estimated defocus

##### Voltage, current and power

In-orbit HRS voltages, currents and power consumptions, identical to predictions and on-ground measurements, exhibit stable behaviour, demonstrating the good health of the instrument

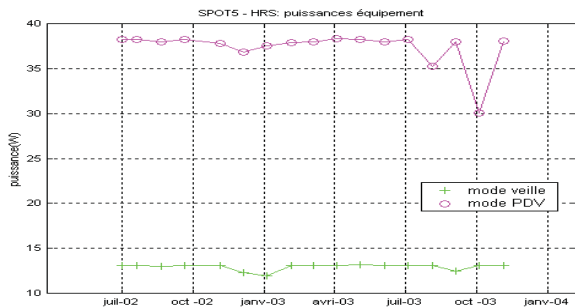


Fig.13: HRS power consumption on BNR/CU in imaging and stand-by modes

##### Temperatures

The in-orbit thermal control is performing as expected. The only unexpected behaviour concerns the CCD proximity electronics slightly hotter than predicted due to a higher satellite interface on -Xs side. Nevertheless this result has no performances impact.

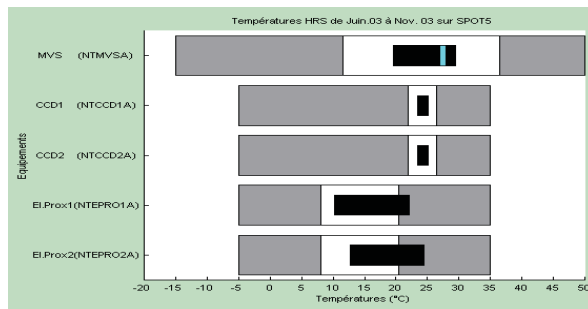


Fig.14 : In-orbit HRS electronics temperature (black) versus operational (white) and non-operational (grey) temperature ranges

As expected, no long-term thermal evolution is observed on cameras, the main contributor remaining the orbital environment:

- Cameras:
  - Orbital temperature stability better than  $\pm 0.2^\circ\text{C}$
  - Orbital gradient stability better than  $\pm 0.5^\circ\text{C}$
- CCD:
  - Orbital temperature stability better than  $\pm 0.8^\circ\text{C}$

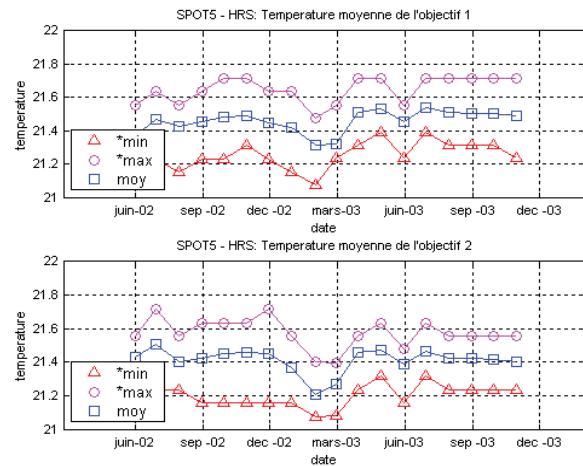


Fig.15: In-orbit telescope temperature

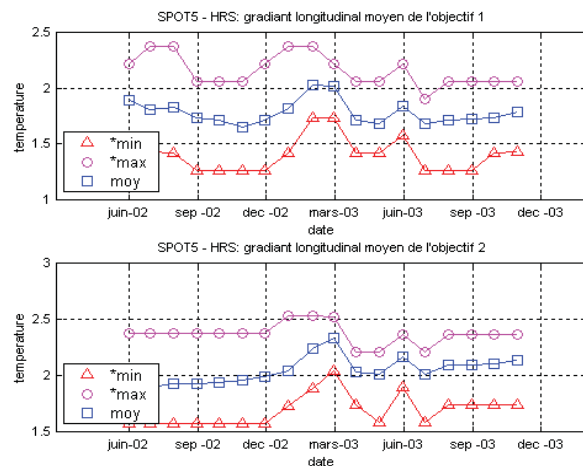


Fig.16: In-orbit telescope longitudinal gradient

##### In-orbit defocus estimation

Considering the correlated defocus model established during on-ground verification, the estimated in-orbit defocus, illustrated on Fig.17, is:

- Camera1 (fore camera):  $[-4\ \mu\text{m}; +16\ \mu\text{m}]$
- Camera2 (aft camera):  $[-3\ \mu\text{m}; +15\ \mu\text{m}]$

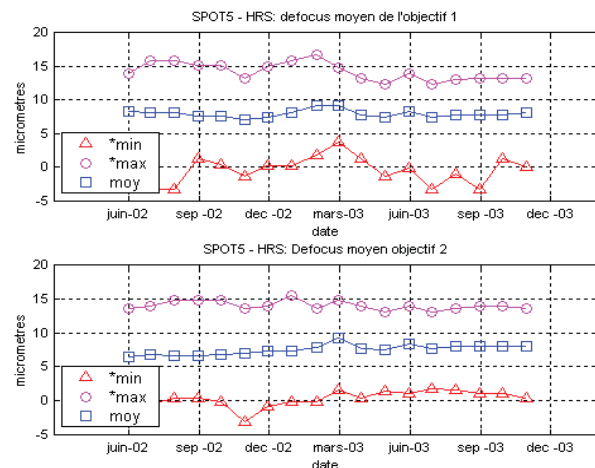


Fig.17: In-orbit HRS instrument estimated defocus

The orbital stability, better than expected ( $\pm 7 \mu\text{m}$  compared to  $\pm 14 \mu\text{m}$ ), can be explained by the inaccuracy of the defocus model heat sink coefficients estimation, inaccuracy due to the impossibility to simulate on-ground the real heat sink (thermal shroud and optical ground support equipment disturbing the representativity of the observed scene during TB/TV).

### In-orbit MTF estimation

From the estimated in-orbit defocus, the worst-case MTF over the field of view is:

- Camera 1: MTF higher than 0.22
- Camera 2: MTF higher than 0.29

much better than the required 0.18 specification.

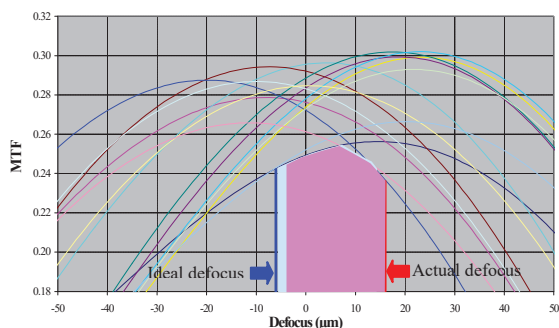


Fig.18: In-orbit MTF with actual and ideal defocus (fore camera)

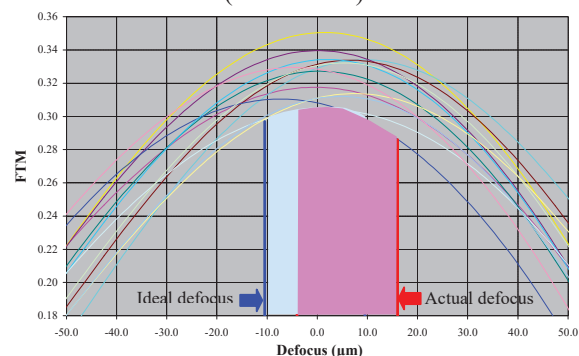


Fig.19: In-orbit MTF with actual and ideal defocus (aft camera)

The analysis of the in-orbit MTF (Fig.18 and Fig.19) demonstrates the good focus adjustment. Indeed, The focus setting is found close to the optimum ( $-2 \mu\text{m}$  on fore camera and  $-6.5 \mu\text{m}$  on aft camera).

Over the 1.5-year in-orbit lifetime, all parameters are stable and exhibit excellent performances.

### 3.2. HRS Acquisition

Since May 2002 systematic HRS acquisition is planned over pre-determined area that are classified depending of strategic and commercial priorities. HRS resource is shared between defence and commercial requirements on the basis of the initial public private partnership risk-sharing scheme:

- 48% defence
- 52% commercial

Acquisition is being processed successfully and overall acquired area exceeds by a factor 3 the original budgets. Data validation is a several steps process:

- Cloud coverage check quickly after acquisition, in order to reallocate satellite resource
- Fine correlation verifications in order to qualify the stereo pairs and to archive them for further potential DEM generation.

Last September 2003, HRS acquisition resulted in 42000000 km<sup>2</sup> of cloud free covered area and 35000000 km<sup>2</sup> of correlated stereo pairs ready for DEM manufacturing.

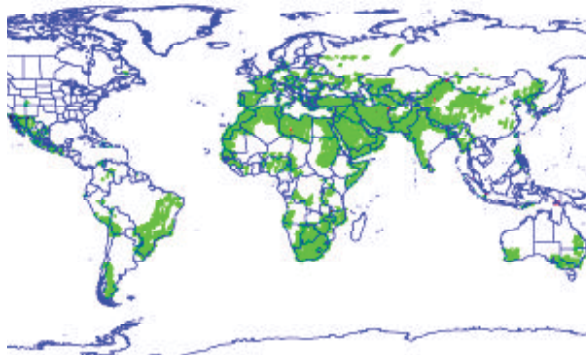


Fig.20: September 2003 cloud free HRS acquisition (green)

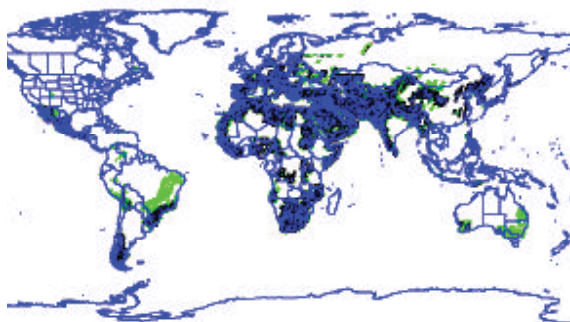


Fig.21: September 2003 HRS correlated stereo pairs (blue)

## 4. HRS DEM PRODUCTS

### 4.1. REFERENCE3D

Reference3D, the HRS Digital Elevation Model (DEM) commercial product, is produced under a co edition agreement between France's Institut Géographique National (IGN) and Spot Image. It is a tiled product, complete geographical information source, made up of one-degree square tiles containing 7 geographically superposable layers:

- A DEM layer
- An ortho image layer
- Seven "quality" layer including source data used for DEM and ortho image, quality indicators on those data, DEM masks and accuracy figures.

#### 4.2. HRS DEM Performances<sup>(2)</sup>

Location performances resulting from heavy work of French space agency (CNES) and mapping agency (IGN), has been conducted on more than 20 test sites.

Reference3D production process is based on three steps:

- Registration of stereo pairs
- Generation of a DEM by automatic correlation on the stereo pairs
- Overall calculation of absolute site geometry by block triangulation

First level accuracy is mainly affected by orbital performances. Nevertheless, elevation accuracy (z) is already better than 15m for more than 90% of points.

Table5: Raw location performance

	Cross track	Along track	z
<b>Mean</b>	-0.7 m	-3.7 m	-5.6 m
<b>Standard deviation</b>	18.7 m	34.3 m	7.4 m
<b>90% threshold</b>	62.4 m		14.5 m

Modelling of thermo elastic effect resulting from orbital position reduces significantly location dispersion. Block triangulation, most effective part of correction, increases planimetric accuracy by more than a factor 2 on planimetry and than a factor 3 on elevation accuracy.

Table6: Location performance after thermo elastic effects modelling and correction and block triangulation

	Cross track	Along track	z
<b>Mean</b>	0.5 m	0.5 m	-0.7 m
<b>Standard deviation</b>	6.4 m	5.2 m	2.6 m
<b>90% threshold</b>	12.3 m		4.0 m

Finally, elevation accuracy can still be improved, using elevation data of known points in the block triangulation process, that has sense as coastlines provide simple accurate potential points at zero elevation.

Table7: Location performance after block triangulation with Z control points

	Cross track	Along track	z
<b>Mean</b>	-0,3 m	0,5 m	0,0 m
<b>Standard deviation</b>	7,2 m	5,1 m	0,7 m
<b>90% threshold</b>	13,4 m		1,2 m

This evaluation campaign and the continuous in orbit monitoring have confirmed that the Reference3D users needs are satisfied and somewhat exceeded. This will allow providing satellite data with high location performances all over the world avoiding necessary use of Geographical Control Points (GCP).

#### 5. CONCLUSION

The HRS instrument, funded via an innovative private/public partnership, was developed in two years as originally planned with a mono model philosophy. The on-ground and in-orbit performances exceed the instrument requirements and satisfy the HRS mission.

Indeed, the HRS acquisition is today in advance with respect to the original acquisition plan and the DEM products exhibit outstanding performances after compensation (1 m compared to 10 m requirement).

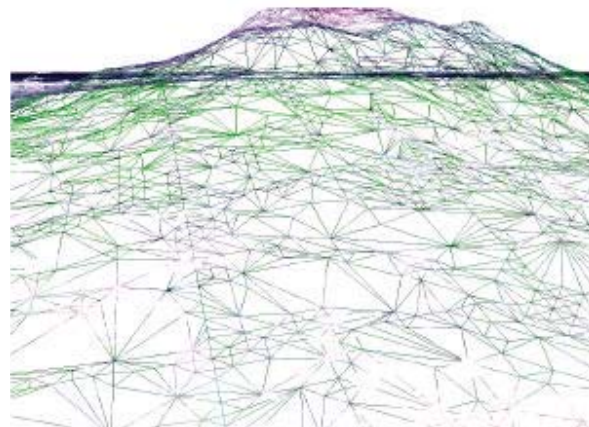


Fig.22: HRS Digital Elevation Models (Vesuvio)

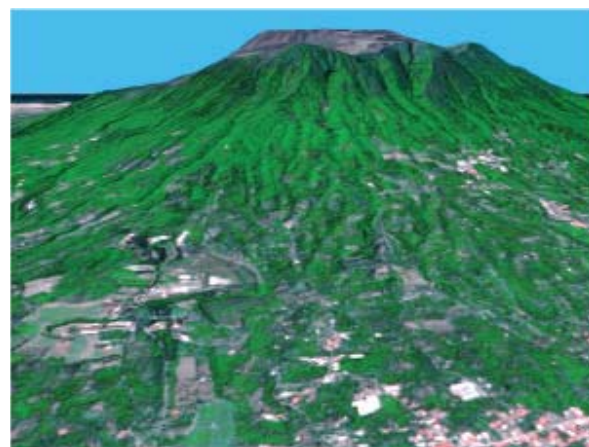


Fig.23: Vesuvio 3D view derived from SPOT5

#### 6. ACKNOWLEDGEMENTS

The HRS mission success is the result of efforts spent to conduct the instrument development and then produce the Digital Elevation Models.

The authors wish to thank all people at CNES, ASTRIUM, SPOTIMAGE, IGN who contributed by their daily work to the success of this mission.

#### 7. REFERENCE

- (1) Laurent Maggiori, Christian Rouziès, Marc Bernard, "HRS: an enhanced mission capability for SPOT5", AIAA, 2000
- (2) Reference3D location performance review and prospects *ISPRS & EARSEL joint Workshop "High-Resolution Mapping from Space 2003"*, Hanover, Germany
- (3) Laurent Maggiori, Michel Duran, Gilles Planche, "HRS: a first assessment", IAF, 2003